Energy Conversion and Management 87 (2014) 351–358

Contents lists available at ScienceDirect

Energy Conversion and Management

journal homepage: www.elsevier.com/locate/enconman

Investigation of turbidity effect on exergetic performance of solar ponds

Ayhan Atiz [a], Ismail Bozkurt [b], Mehmet Karakilcik [a,*], Ibrahim Dincer [c]

[a] Department of Physics, Faculty of Sciences and Letters, University of Cukurova, Adana 01330, Turkey
[b] Department of Mechanical Engineering, Faculty of Engineering, University of Adiyaman, Adiyaman 02040, Turkey
[c] Faculty of Engineering and Applied Science, University of Ontario Institute of Technology (UOIT), 2000 Simcoe Street, North Oshawa, Ontario L1H 7K4, Canada

ARTICLE INFO

Article history:
Received 16 April 2014
Accepted 4 July 2014

Keywords:
Solar pond
Turbidity effect
Transmission of salty water
Exergy analysis
Efficiency

ABSTRACT

The present paper undertakes a study on the exergetic performance assessment of a solar pond and experimental investigation of turbidity effect on the system performance. There are various types of solar energy applications including solar ponds. One of significant parameters to consider in the assessment of solar pond performance is turbidity which is caused by dirty over time (e.g., insects, leaf, dust and wind bringing parts fall down). Thus, the turbidity in the salty water decreases solar energy transmission through the zones. In this study, the samples are taken from the three zones of the solar pond and analyzed using a spectrometer for three months. The transmission aspects of the solar pond are investigated under calm and turbidity currents to help distinguish the efficiencies. Furthermore, the maximum exergy efficiencies are found to be 28.40% for the calm case and 22.27% with turbidity effects for the month of August, respectively. As a result, it is confirmed that the solar pond performance is greatly affected by the turbidity effect.

1. Introduction

Turkey has high solar energy potential because of its location in the northern hemisphere with latitudes 36–42° N and longitudes 26–45° E. This makes it worth to investigate and conduct research on this solar energy source [1]. One system to collect and store solar energy is solar pond which can be used to supply thermal energy for various applications, such as process and space heating, water desalination, cooling, drying and possibly power generation [2]. A solar pond is considered a low cost solar energy system which collects solar radiation and stores it as thermal energy in the same medium for a long period of time [3]. Many studies have been carried out to increase the performances of solar ponds. In salt gradient solar ponds, the clarity of water and absorptivity of the bottom are important concerns. Turbidity hinders the propagation of radiation. Thereby it decreases the flux reaching the storage zone [4].

Solar energy is received as both direct and diffuse radiation and distributed primarily over the wide range of the ultraviolet, visible and infrared spectra. A higher radiation transmission through the upper zone and gradient in a solar pond results in a higher heat collection efficiency [5]. Studying the decreasing effect of solar radiation with depth through a simple empirical model was presented [6]. A novel two-layer nanofluid solar pond has been investigated theoretically that describes the thermal performance of the solar pond. In this study, they have been achieved by improving the thermal efficiency and the storage capacity by using nanofluid in order to increase the extinction coefficient of the lower layer of the pond [7].

Solar spectrum divided into 40 parts and came to the result that four parts also give reasonable accuracy in transmittance predicts used for modeling the thermal performance of solar pond [8]. The attenuation of light in the clearest natural waters, solar pond and salt water has been varied. Irradiance just not depend on water and salty. There is another important thing impact, we know this is turbidity and common problem encountered in salinity-gradient solar ponds is the growth of various types of algae and bacterial populations which affects the brine clarity and hence reduces thermal performance [9]. A solar pond as a solar collector is dependent on light transmission to the storage zone. Clarity of the brine is one of the most important factors in achieving good thermal performance and stability the higher the transparency the better the performance [10]. A theoretical model for solar pond to investigate the turbidity in water was presented, and they showed turbidity very important reducing solar radiation in water [11]. The combined effect of the bottom's reflectivity and water turbidity on the steady state efficiency of solar ponds were investigated. It was found that in the case of a reflective bottom, turbidity, within certain limits, improves the efficiency of pond [12].

* Corresponding author.
E-mail addresses: kkilcik@cu.edu.tr, mehmet01_karakilcik@hotmail.com (M. Karakilcik).

http://dx.doi.org/10.1016/j.enconman.2014.07.016
0196-8904/

Nomenclature

a	absorption coefficient
b	thickness of the solution (m)
C	heat capacity (J/kg °C)
Ex	exergy (MJ)
F	absorbed energy fraction at a region of δ-thickness
HSZ	heat storage zone
h	transmission rate
I	solar beam
m	mass (kg)
n	number of the parts
NCZ	non-convective zone
s	salinity (g/kg)
S	entropy (J/K mol)
T	temperature (°C)
t	transmission coefficient
Q	heat (J)
UCZ	upper convective zone
V	volume (m^3)
z	depth

Greek letters

ε	molar absorption coefficient
θ	angle
ρ	density (kg/m^3)
β	incident beam entering rate into water
λ	wavelength (nm)
μ	absorbing coefficient
ψ	exergy efficiency
η	energy efficiency

Subscripts

dest	destruction
g	gain
in	incidence
ref	refraction
surr	surrounding
sys	system

In this paper, we in general investigate the effect of turbidity on the performance of the pond through exergy efficiency. The specific objectives are to study both experimentally and theoretically for two cases under, namely calm conditions and turbidity currents and determine energy and exergy contents and compare their exergy efficiencies for three different zones (layers) of the ponds. Note that a solar pond consists of three different density zones, such as Upper Convective Zone (UCZ), Non-Convective Zone (NCZ) and Heat Storage Zone (HSZ). The zones' density increases from top to bottom of the pond. Each of the zones is important and affects the performance of the overall performance of the pond.

2. Experimental system

Fig. 1 illustrates the inner zones of the solar pond along with the exergy flows. The first zone, Upper Convective Zone (UCZ), is the fresh water layer at the top of the pond. This zone is fed with fresh water in order to maintain its density as close as to the density of fresh water. The second zone is the Non-Convective Zone (NCZ) between the Heat Storage Zone (HSZ) and UCZ. The NCZ is composed of salty water layers whose brine density gradually increases toward HSZ. NCZ is the key to the working of a solar pond. The third zone (HSZ), which is known as heat storage zone, is composed of salty water with the highest density. Considerable part of the solar energy is absorbed and stored by this bottom region [13]. In this study, we used two solar ponds as turbid pond and clean pond in Cukurova University in Adana, Turkey (i.e., 35° 18′ E longitude 37° 05′ N latitude). These two solar ponds were tested in parallel during the experiments. The turbid pond was kept dirty after a year due to the surround environmental factors, particles, algae and bacterial populations. The new and clean one was filled by using clean salty solution. Afterward, the samples are taken from the zones of the solar pond and analyzed by using spectrometer for three months. The experimental temperature distributions were measured by using thermocouples which were placed into the inner zones of the solar pond. The solar pond is filled up with salty water. HSZ is started from the bottom of the pond until 0.80 m height and its density approximately 1180 kg/m^3 with salt water. The middle zone, NCZ is composed of salty water layers whose brine density gradually increases toward HSZ. NCZ is formed five layers at different concentrations top on the HSZ. The thickness of each layer is 0.20 m and layers' density are decreasing from HSZ to UCZ. The decreasing between 1100 and 1015 kg/m^3 as graded for each layer. So, these constitute non-convective zone as salty gradient zone. The surface zone, UCZ is the fresh water layer at the top of the pond. The inner zones (UCZ, NCZ and HSZ) are maintenance, density distributions, sustainability of salinity gradient and salty water clarity are of key important for heat storage performance of the solar pond. Therefore, especially, the protection of density distributions of the zones and its cleanliness are requires maintenance, continuously. For this purpose, we put 10 unit transparent plastic hoses which are 5 mm diameter with 0.20 m distance on 2 m length and board in the pond to measure the density distributions of the solar pond. The salty water samples

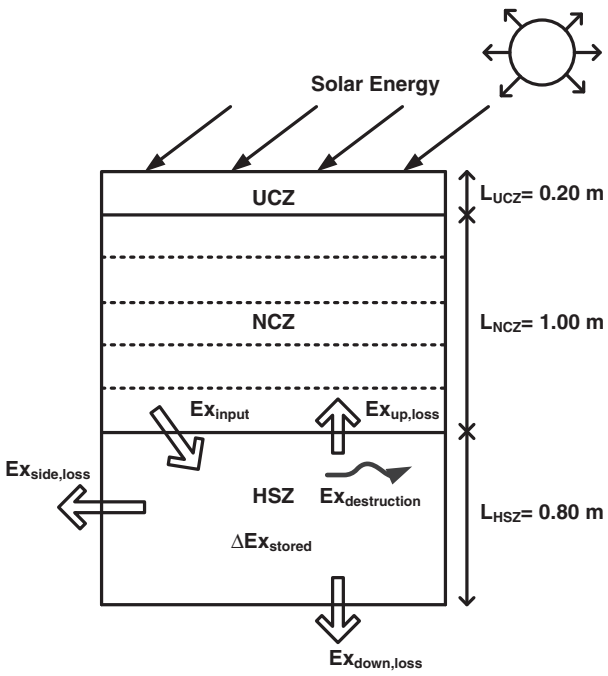

Fig. 1. The inner zones of the solar pond and exergy fluxes.

of the layers are taken through the hoses to measure the density and transmission of the turbid and clean salty water by using hydrometer and spectrometer, separately.

A hydrometer is used manually to measure the density of the liquids samples. It consists of a thin elongated cylindrical glass bulb. Thin side is included a scale as metric to measure the relative density of the samples. Cylindrical glass bulb side is weighted with small lead balls to make it float upright when immersing it to sink in the saline water container which cylinder has a 250 ml capacity.

A spectrometer is an instrument used to measure properties of light over a specific portion of the electromagnetic spectrum [14]. The measurement samples contained a solution of distilled water and of normal grade salt. The following salts were studied: $MgCl_2$, Na_2SO_4, $NaNO_3$, KNO_3 and Na_2CO_3. The transmission spectra were measured with a spectrometer in the range 300–1200 nm. The quartz–glass sample containers of 50 mm length were of good quality [15].

3. Analysis

3.1. Solar radiation coefficients

The incident flux of solar radiation reaching the surface of the pond gets partially reflected and the remainder penetrates into the pond and also propagates through the body of the pond gets attenuated in its path. It is a recognized the fact that solar radiation attenuation is one of the most important parameters affecting the thermal performance of a salt gradient solar pond. However, it is difficult to obtain the attenuation curve experimentally, due to lack of availability of accurate under-water pyrometers. Thus, a solar radiation attenuation model is usually adopted in computer simulation of solar pond performance [16]. The solar radiation absorption that takes place in most natural waters is attributable to three components such as the water itself, dissolved organic matter, variously referred to as yellow substance [17]. In order to increase the solar radiation input owing into the storage zone of the solar pond, NCZ and UCZ must be transparent as possible as because both the intensity of incident ray and the absorption of salt-water solution depend on the wavelength to calculate the total transmittance precisely [18]. Most of the solar radiation in the near infrared spectrum is absorbed within the first centimeter of depth of UCZ. The radiation associated with wavelengths greater than 1200 nm represented 22.4% of the total incident radiation and this radiation was totally absorbed in this upper water boundary layer for radiation with $\lambda < 1200$ nm [19]. Radiation emitted by the sun travels through the vacuum of space unaltered. The percentage of energy associated with certain bandwidths of solar radiation emitted from a blackbody at 5800 K (the sun's temperature) [20]. Light entering the pond is also scattered by the various suspended particles. The scattering particles however are assumed not to absorb energy [21]. The solar absorption of a partially transparent medium follows the Bouguer's law, which is based on the assumption that the absorbed radiation is proportional to the local intensity in medium and the distance b that radiation has traveled inside the medium and transmission of the light is given as:

$$dI = (-\mu I)db \tag{1}$$

where dI is the change in intensity across db, db is the thickness of the medium as we integrate over Eq. (1):

$$\int_{I_0}^{I} \frac{dI}{I} = -\mu \int_0^b db \tag{2}$$

Here, I is equal the percentage transmittance of intensity of the radiation. The percentage transmission is expressed in terms of an absorbance which is defined by Beer–Lambert law:

$$\%T = In\frac{I}{I_0} = \mu b \tag{3}$$

and the absorption coefficient is given as:

$$\mu_i = b^{-1}[\%T]_i \tag{4}$$

where b is the thickness of the solution in quartz–glass tube of spectrometer. The thickness of the quartz tube is $b = 0.5$ cm. $\%T$ is the percent transmittance of the salty water samples which are taken from the layers of the solar pond. The layer numbers from top to bottom are $i = 1$–10. Each sample was analyzed by using the UV/VIS spectrometer between 400 and 700 nm wavelength. The absorption coefficient (μ) was calculated for three different wavelength ranges as 400–500, 500–600 and 600–700 nm, respectively. The experimental transmission measurements were obtained by using spectrometer. The absorption coefficients were calculated using Eq. (4). Thus, the absorption coefficients (μ) were found for different layers as seen in Table 1. Thus, the molar absorption coefficients (ε) were calculated to found transmission for each layer of the clean and turbid water of the pond for three months. The transmission equation is given in a logarithmic function form:

$$\log\left(\frac{I}{I_0}\right) = -\frac{\mu}{2.30}b \tag{5}$$

with the absorption function as:

$$A = \varepsilon cb = \log\left(\frac{I}{I_0}\right) \tag{6}$$

By equalizing Eqs. (5) and (6), the extinction coefficient depends on multiplying molar absorption coefficient (ε) and concentration:

$$\varepsilon c = \frac{\mu}{2.30} \tag{7}$$

Now, the general molar absorption coefficient is given as:

$$\varepsilon = 0.43\sum_{i=1}^{n}\frac{\mu_i}{c_i} \tag{8}$$

The general total molar absorption coefficient that is specific for each solution for clean and turbid water cases is written by using Eqs. (5) and (10):

$$\varepsilon = 0.43\sum_{i=1}^{n}\frac{b^{-1}[\%T]_i}{c_i} \tag{9}$$

where n is the number of measurement of the samples for three different wavelength range. c is the concentration which is calculated using the experimental data for each layer.

The attenuation of radiation through a pure medium is described by the Bouguer–Beer law; to measured solar energy with the depth, giving the Lambert–Beer law that depends on wavelength λ and way, ray of light intensity in the depth (z):

$$I_{i+1}(z) = I_i e^{-\mu_i(\lambda)z} \tag{10}$$

where $I_{i+1}(z)$ is the wave length (λ) bunch of the beam with the depth (z). I_i is entered the water all part of solar energy and $\mu(\lambda) = -1/\delta(\lambda)$, $\delta(\lambda)$ is characteristic of absorbing coefficient:

$$\sum_{i=0}^{10} I_{i+1}(z) = \sum_{i=0}^{10} I_i e^{-\mu_i(\lambda)z} \tag{11}$$

The equation can written as the transmission rate $h_{i+1}(z-\delta)$ below:

$$h_{i+1}(z-\delta) = \frac{\sum_{i=0}^{n=10} I_i e^{-\mu_i(\lambda)z}}{\sum_{i=0}^{n=10} I_{i+1}(z)} \tag{12}$$

Table 1
The optical parameters of turbid and clean water samples of the different layers of the pond for the month of August.

I	z (cm)	Turbid water			Clean water		
		c (kg/m^3)	μ	ε	c (kg/m^3)	μ	ε
1	20	0.025	0.0023546	0.0408604	0.005	0.0010101	0.0876473
2	40	0.029	0.0029134	0.0435851	0.020	0.0031589	0.0685238
3	60	0.066	0.0046545	0.0305957	0.035	0.0033721	0.0417981
4	80	0.100	0.0079112	0.0343219	0.050	0.0068433	0.0593749
5	100	0.140	0.0085479	0.0264887	0.075	0.0071555	0.0413885
6	120	0.163	0.0158169	0.0420980	0.100	0.0092702	0.0402176
7	140	0.179	0.0291573	0.0706681	0.130	0.0162711	0.0543004
8	160	0.180	0.0228708	0.0551237	0.150	0.0202733	0.0586356
9	180	0.180	0.0285602	0.0688363	0.180	0.0212442	0.0512031
10	200	0.181	0.0178837	0.0428656	0.180	0.0062582	0.0150835

3.2. Exergy analysis

Exergy analysis is a method that uses the conservation of mass and conservation of energy principles together with the second law of thermodynamics for the analysis, design and improvement of energy and other systems [22]. The exergy values of the solar pond are calculated by using conservation of mass and energy principles as well as second law analysis. The exergy balance equations are the most essential key to know the thermal behavior of solar ponds. The exergy balance equation of a solar pond is written as

$$\Delta Ex_{stored} = \sum_{i=6}^{10} Ex_{(i+1)} - (Ex_{dest,HSZ} + Ex_{up,loss} + Ex_{side,loss} + Ex_{down,loss}) \tag{13}$$

Here, $Ex_{(i+1)}$ is the exergy input to HSZ for $(i+1)$ layer, $Ex_{dest(i+1)}$ is the exergy destruction in HSZ, $Ex_{up,loss}$ is the exergy loss from HSZ to NCZ, $Ex_{side,loss}$ is the exergy loss through side walls. $Ex_{down,loss}$ is the exergy loss through bottom wall and also, Ex_{stored} is the exergy stored in HSZ.

$$Ex_{i+1} = \beta Ex_{solar} A_{HSZ}[(1-F)h_{i+1}(z-\delta)] \tag{14}$$

where β is the fraction of the incident solar incident that actually enters the pond [23]:

$$\beta = 1 - \left[\frac{\sin\theta_{in} - \sin\theta_{ref}}{\sin\theta_{in} + \sin\theta_{ref}}\right] - 0.4\left[\frac{\tan\theta_{in} - \tan\theta_{ref}}{\tan\theta_{in} + \tan\theta_{ref}}\right] \tag{15}$$

Here, θ_{in} and θ_{ref} are the incidence angle and the refraction angle.

The exergy of solar radiation is expressed as follows [24]:

$$Ex_{solar} = I_{net}\left\{1 - \frac{4T_0}{3T} + \frac{1}{3}\left(\frac{T_0}{T}\right)^4\right\} \tag{16}$$

where I_{net} is the net solar radiation coming on the surface of pond.

For example; the first layer's number of HSZ, Ex_7 is the exergy on the surface of the HSZ for the depth $z = 120$ cm and layers $i = 6$ according to Eq. (6) and is given as

$$Ex_7 = \beta Ex_{solar} A_{HSZ}[(1-F)h(120-\delta)] \tag{17}$$

$$E_{dest,HSZ} = \sum_{i=6}^{10} Ex_{dest(i+1)} = T_0 \sum_{i=6}^{10} (\Delta S_{net,(i+1)}) \tag{18}$$

where $\Delta S_{net,(i+1)}$ is the net entropy change of $(i+1)$ layer which is defined $\Delta S_{net,(i+1)} = \Delta S_{sys} + \Delta S_{surr}$. Then, the exergy losses, including exergy destructions, within HSZ can be derived as follows:

$$Ex_{dest,HSZ} = T_0\left[m_{HSZ}C_{p,HSZ}\ln\left(\frac{T_{HSZ}}{T_0}\right) - \left(\frac{Q_{g,HSZ}}{T_{HSZ}} + \frac{Q_{side,HSZ}}{T_0}\right) + \left(\frac{Q_{down}}{T_0}\right)\right] \tag{19}$$

$$Ex_{up,loss} = m_{HSZ}C_{p,HSZ}\left[(T_{HSZ} - T_{m,NCZ}) - T_0\ln\left(\frac{T_{HSZ}}{T_{m,NCZ}}\right)\right] \tag{20}$$

where $m_{HSZ} = \rho_{HSZ}V_{HSZ}$ is the mass of salty water in HSZ; ρ_{HSZ} is the averaged density of HSZ, and V_{HSZ} is the volume of the salty water in HSZ. $C_{p,HSZ}$ is the specific heat of HSZ; T_0 is the reference environment temperature; T_{HSZ} is temperature of HSZ and $T_{m,NCZ}$ denote the average temperature of NCZ. The specific heat capacity and salinity of the zones was calculated by using an empirical equation as given in Eq. (21) [25]:

$$C = (-0.0044s + 4.1569)1000 \tag{21}$$

Here, C is heat capacity (J/kg °C) and s is the salinity (g/kg). The density difference at low temperature takes place approximately in linear relationship between density and salinity. We use an empirical correlation as given in Eq. (12) and calculate the salinity of the zones as follows:

$$s = \frac{(\rho - 998.24)}{0.756} \tag{22}$$

Furthermore, $Ex_{down,loss} = Ex_{side,loss}$ due to the fact that both side wall and bottom layer have the same insulating materials and are surrounded by the ambient air, as follows:

$$Ex_{side,loss} = m_{HSZ}C_{p,HSZ}\left[(T_{HSZ} - T_0) - T_0\ln\left(\frac{T_{HSZ}}{T_0}\right)\right] \tag{23}$$

We can now define the exergy efficiency for HSZ as the ratio of the exergy stored in HSZ to the total exergy input to HSZ:

$$\psi = \frac{Ex_{stored}}{\sum_{i=6}^{10} Ex_{(i+1)}} = 1 - \frac{(Ex_{dest,HSZ} + Ex_{up,loss} + Ex_{side,loss} + Ex_{down,loss})}{Ex_{HSZ}} \tag{24}$$

3.3. Energy analysis

The thermal performance of the solar pond system was calculated by using the energy balance equation. In this study, we focus on the heat flux in HSZ because the useful heat energy is stored in HSZ. All calculations for the energy and exergy values were done hourly basis. The convection and radiation heat loss in the solar pond were neglected. The energy balance equation is written as below:

$$Q_{stored} = Q_{solar,HSZ} - Q_{loss,HSZ} = \beta EA[(1-F)h(x-\delta)] - \left\{\frac{k_s A}{\Delta x_{HSZ-NCZ}}(T_{HSZ} - T_{NCZ}) + \frac{k_{sw}2\pi r L_{HSZ}}{\Delta x_{side}}(T_{HSZ} - T_a) + \frac{k_{sw}A}{\Delta x_{down}}(T_{down} - T_a)\right\} \tag{25}$$

where E is the solar energy reaching the surface, A_{HSZ} is the area of the HSZ, F is the fraction of energy absorbed at a region of δ-thickness, h is the solar radiation ratio, A is the surface area, T_a is the air temperature, k_{sw} is the thermal conductivity of the walls, k_s is the thermal conductivity of the salty water, L_{HSZ} is the thickness of the HSZ, r is inner radius of the cylindrical solar pond, Δx_{down} is

the thickness of the down wall, Δx_{side} is the thickness of the side wall, $\Delta x_{HSZ\text{-}NCZ}$ is the thickness of the HSZ's middle point and the NCZ's middle point, and β is the fraction of the incident solar radiation. The energy efficiency of the solar pond can be defined as:

$$\eta = 1 - \frac{\left\{\frac{k_s A}{\Delta x_{HSZ-NCZ}}(T_{HSZ} - T_{NCZ}) + \frac{k_{sw} 2\pi r L_{HSZ}}{\Delta x_{side}}(T_{HSZ} - T_a) + \frac{k_{sw} A}{\Delta x_{down}}(T_{down} - T_a)\right\}}{\beta E A[(1-F)h(x-\delta)]} \quad (26)$$

4. Results and discussion

A solar pond is used to store the heat energy in the bottom zone of the solar pond. The first part of the experiment is carried out to determine the temperature and density variation of the solar pond. In the second part of the experiment which is carried out to turbidity effect on the performance of the solar pond by using a spectrometer. The comparison of the density distribution is shown in Fig. 2 for the turbid and clean water of the solar pond. As shown in Fig. 2, the differences of the salinity gradient are kept approximately stable for two different solar ponds.

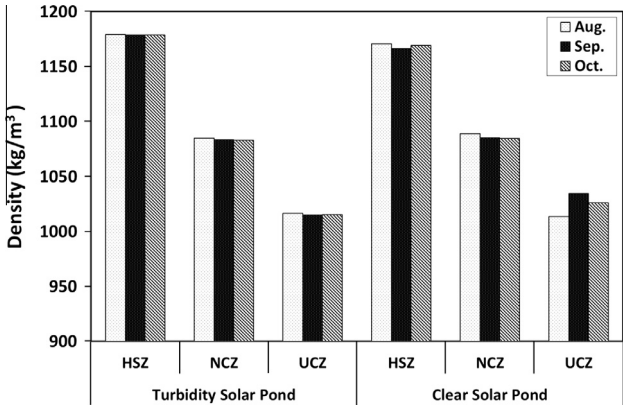

Fig. 2. The comparison of the density distribution for turbid and clean water of the solar pond.

Tables 1, 2 and 3 list the optical parameters such as absorption coefficient (m) and molar coefficient (e) of turbid and clean water samples of the different layers of the pond for the months of August, September and October. These parameters were calculated by using the experimental transmission data, average concentration and thicknesses of each layer (Eqs. 4 and 9). Table 4 lists the mass, volume, specific heat capacity and turbidity for the clear and turbidity solar pond. The specific heat capacity is calculated by using density and salinity in Eq. (21). The turbidity of the zones in the solar pond was measured by using Photometer Nanocolor 100 D. The range of the Photometer Nanocolor is 1–100 ntu. The measurements were done in 620 nm wavelength. As seen in Table 4, the turbidity in the solar pond is increasing with time. The increasing turbidity is accumulated in the storage zone of the solar pond. The transmission in the solar pond decreases with the increase of the turbidity, gradually.

The monthly total global solar energy and exergy is given in Fig. 3 for Adana, Turkey. As seen in Fig. 3, the maximum total solar energy in Adana is 713.91 MJ in June, while the minimum is 218.48 MJ in January. Solar exergy is calculated by using Eq. (16). The maximum total solar exergy in Adana is 666.32 MJ in June, while the minimum is 204.77 MJ in January.

Fig. 4 demonstrates the comparison of the temperature distribution for turbidity and clear solar pond. The temperature of the solar pond was affected by turbidity due to decrease of the solar radiation reaching to HSZ. As seen in Fig. 4, firstly for turbid water of the solar pond, the temperature of UCZ is observed to peak at 30.33 °C in August and the temperature is dropped at 21.40 °C in October. Similarly, the temperature of NCZ is observed to peak at 40.15 °C in August, and is dropped at 27.78 °C in October. While the temperature of HSZ is observed to be maximum at 41.87 °C in August and minimum at 32.72 °C in October. Secondly, for the clean water of the solar pond; the temperature of UCZ is observed to be maximum at 30.30 °C in August, a minimum at 21.91 °C in

Table 2
The optical parameters of turbid and clean water samples of the different layers of the pond for the month of September.

I	z (cm)	Turbid water			Clean water		
		c (kg/m^3)	μ	ε	c (kg/m^3)	μ	ε
1	20	0.021	0.0030937	0.0639142	0.004	0.0015229	0.1651800
2	40	0.023	0.0027329	0.0515499	0.020	0.0026461	0.0573995
3	60	0.061	0.0047093	0.0334935	0.033	0.0045485	0.0597987
4	80	0.100	0.0087470	0.0379482	0.050	0.0070178	0.0608925
5	100	0.151	0.0097078	0.0278915	0.076	0.0058036	0.0331294
6	120	0.171	0.0168236	0.0426827	0.100	0.0151593	0.0657670
7	140	0.171	0.0298918	0.0758378	0.130	0.0187346	0.0625218
8	160	0.180	0.0303067	0.0730460	0.151	0.0159226	0.0457476
9	180	0.181	0.0269498	0.0645961	0.180	0.0235001	0.0566405
10	200	0.181	0.0178837	0.0403245	0.181	0.0228379	0.0547402

Table 3
The optical parameters of turbid and clean water samples of the different layers of the pond for the month of October.

I	z (cm)	Turbid water			Clean water		
		c (kg/m^3)	μ	ε	c (kg/m^3)	μ	ε
1	20	0.021	0.0033604	0.0694233	0.004	0.0020411	0.2213774
2	40	0.021	0.0029177	0.0602773	0.020	0.0032269	0.0699983
3	60	0.063	0.0055079	0.0379296	0.033	0.0040484	0.0532236
4	80	0.100	0.0089896	0.0390006	0.050	0.0085172	0.0739025
5	100	0.151	0.0100335	0.0288274	0.076	0.0077075	0.0439977
6	120	0.170	0.0175698	0.0448383	0.100	0.0155077	0.0672787
7	140	0.180	0.0373607	0.0900475	0.130	0.0175101	0.0584352
8	160	0.181	0.0246238	0.0590209	0.151	0.0171472	0.0492658
9	180	0.181	0.0303067	0.0726424	0.180	0.0225992	0.0544691
10	200	0.181	0.0202732	0.0485930	0.181	0.0168236	0.0403245

Table 4
The mass, volume, specific heat capacity and turbidity for the turbid and clean water of the solar pond.

	Clean water			Turbid water		
	HSZ	NCZ	UCZ	HSZ	NCZ	UCZ
Mass (kg)	1878.52	2182.45	411.81	1894.99	2177.56	408.10
Volume (m^3)	1.60768	2.0096	0.40192	1.60768	2.0096	0.40192
Specific heat capacity (J/kg °C)	3166.16	3646.05	4003.41	3106.52	3660.19	4057.15
Turbidity (ntu)	17	6	5	63	10	6

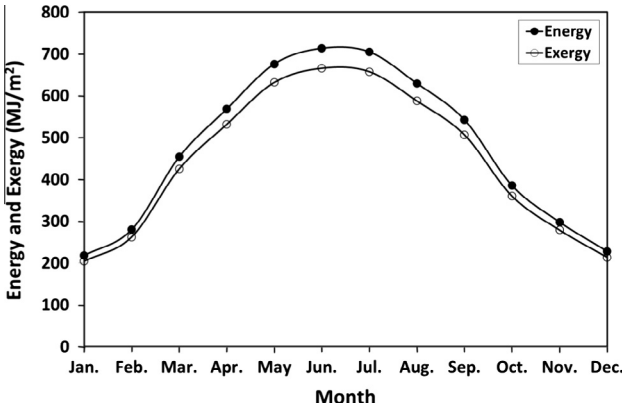

Fig. 3. The monthly total global solar energy and exergy in Adana, Turkey.

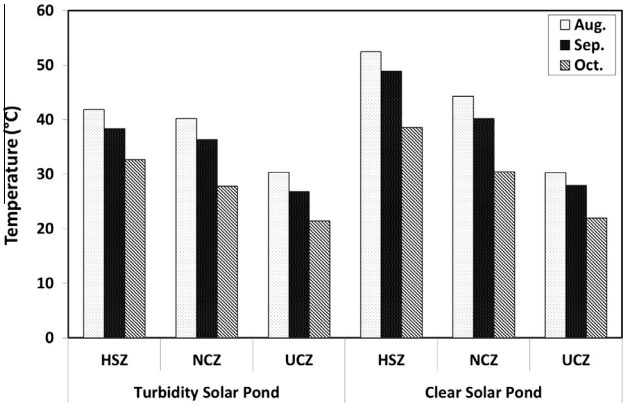

Fig. 4. The comparison of the temperature distributions for turbid and clean water of the solar pond.

October. Similarly, the temperature of NCZ is determined to be maximum at 44.28 °C in August and minimum at 30.45 °C in October, whereas the temperature of HSZ is measured to be a maximum at 52.45 °C in August and minimum at 38.68 °C in October. As expected that the significant temperature increases was obtained for clean water of the solar pond.

The experimental temperature of the clear and turbid solar pond was subjected to the analysis of variance (one-way ANOVA) by using SPSS 15.0 [26] and the Duncan's multiple range tests. These tests were performed to determine the significant differences between the means. Table 5 shows the proximate composition of the experimental temperature with ± standard errors.

The transmission of the layers of the solar pond is determined measuring the turbid and clean water samples by using the spectrometer. The transmission of turbid and clean water samples was correlated with each other. The transmission of the clean and turbid water is shown in Figs. 5–7 for three months. As seen in Fig. 5, the transmission of the solar energy is determined for HSZ of the clean and turbid water as 30.20% and 19.35% in August,

Table 5
Proximate composition of the experimental temperature data with ± standard error for the clear and turbid solar pond.

	Month	Clear $\overline{X} \pm SE$	Turbid $\overline{X} \pm SE$
HSZ	August	52.45 ± 0.265a	41.87 ± 0.284a
	September	48.85 ± 0.578b	38.85 ± 0.532b
	October	38.68 ± 0.632c	32.72 ± 0.623c
NCZ	August	44.28 ± 0.548a	40.15 ± 0.125a
	September	40.95 ± 0.363b	38.36 ± 0.458b
	October	30.45 ± 0.456c	27.78 ± 0.362c
UCZ	August	30.30 ± 0.451a	30.33 ± 0.521a
	September	28.68 ± 0.423b	27.50 ± 0.492b
	October	21.91 ± 0.345c	21.40 ± 0.289c

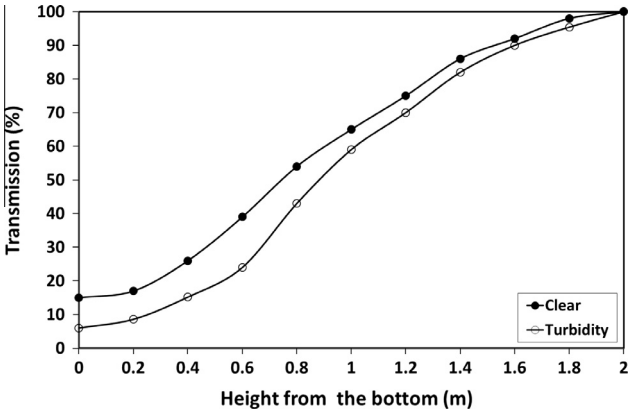

Fig. 5. The transmission of the clear and turbid pond in August.

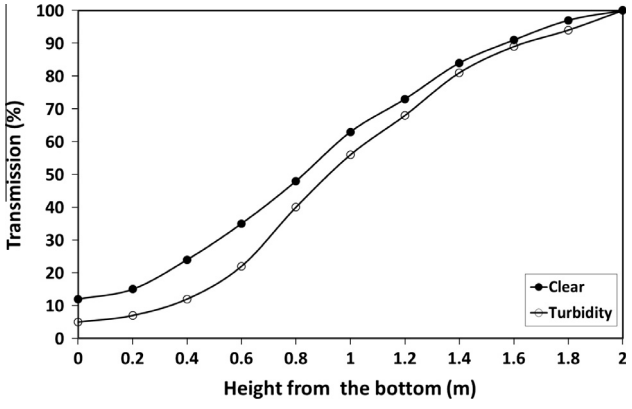

Fig. 6. The transmission of the clear and turbid pond in September.

respectively. As understood from the figure, the reaching solar energy of HSZ is decreased strongly depend on turbidity.

Fig. 6 shows the transmission of solar energy for clean and turbidity pond in September. As seen in Fig. 6, the transmission of the

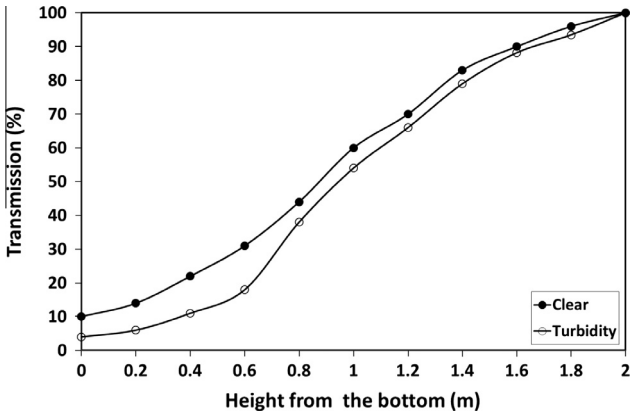

Fig. 7. The transmission of the clear and turbid pond in October.

solar energy is determined for HSZ of the clear and turbidity pond as 26.80% and 17.20% in September, respectively. Similarly, as seen in Fig. 7, the transmission of the solar energy is determined for HSZ of the clean and turbid water of the pond as 24.20% and 15.40% in October, respectively.

Figs. 8 and 9 show the variations of the exergy input, stored, destruction and losses of the clean and turbid water of the pond. As seen in the figures, the exergy stored of the solar pond for clean and turbid water appear to be maximum 63.67 MJ and 33.29 MJ in

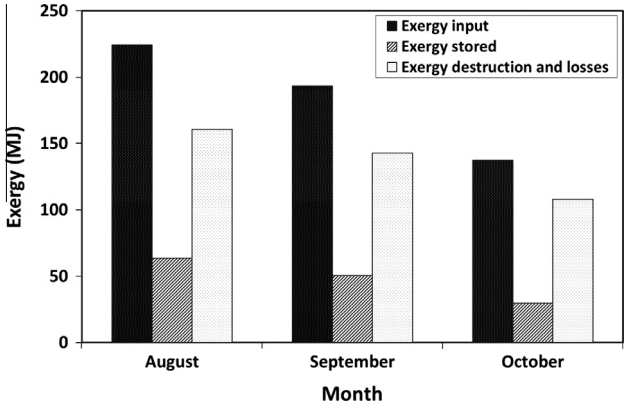

Fig. 8. Variations of the exergy input, stored, destruction and losses of the clean water of the solar pond.

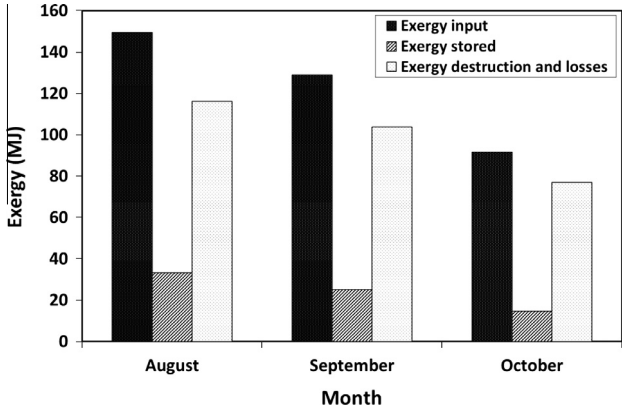

Fig. 9. Variations of the exergy input, stored, destruction and losses of the turbid water of the solar pond.

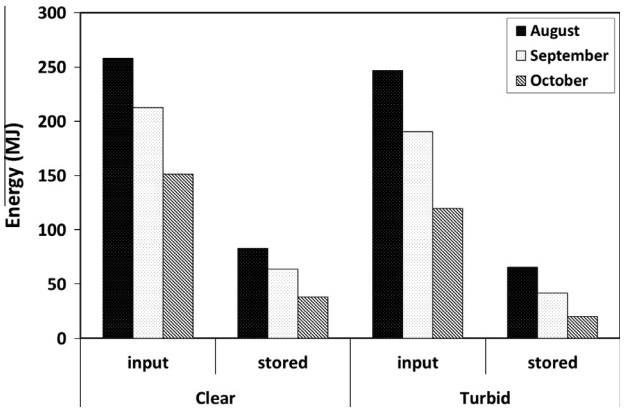

Fig. 10. The comparison of the energy distributions for turbid and clean water of the solar pond.

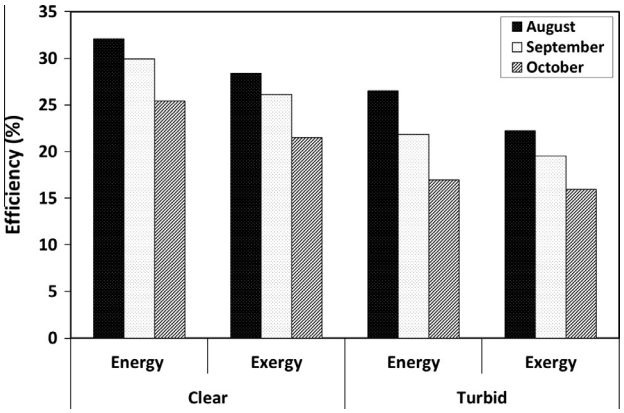

Fig. 11. Energy and exergy efficiencies of the clear and turbid water of the solar pond.

August, and to be minimum 29.58 MJ and 14.65 MJ in October, respectively. As seen in the figures, the exergy input is higher in clean water than turbid water of the pond. The turbidity in the solar pond has negative effect on solar energy transition in the layers.

Fig. 10 shows the comparison of the energy distributions for turbid and clean water of the solar pond. As seen in Fig. 10, the energy stored of the solar pond for clean and turbid water appear to be maximum 82.77 MJ and 65.46 MJ in August, and to be minimum 38.45 MJ and 20.27 MJ in October, respectively. The performance of the solar pond is low because of the reaching solar energy of HSZ is much smaller than the incident solar radiation on the surface. To increase the reaching solar energy of HSZ, the turbidity should be decreased. The energy and exergy efficiencies of the solar ponds are calculated by using Eqs. (24) and (26). As seen in Fig. 11, the maximum energy efficiencies were found to be 32.10% and 26.52% for clean and turbid water in August, respectively. Furthermore, the maximum exergy efficiencies were found to be 28.40% and 22.27% for clean and turbid water in August, respectively. The turbidity of the solar pond has an important effect on energy and exergy efficiency. If the salty water of the solar pond is kept clean, the solar pond stores more energy and exergy.

5. Conclusions

In this study, we employ two solar ponds (one clean and one turbid) to experimentally investigate the turbidity effect on the

solar pond performance through exergy efficiency under various weather conditions and concentrations. In this regard, various thermal and concentration measurements were performed. The molar and absorption coefficients of each layer were calculated using the experimental percentage transmission. The exergetic efficiency of the solar pond is influenced by the molar and absorption coefficients of each layers. The exergy efficiencies are expressed by using exergy balance equations for the inner zones. The following concluding remarks are extracted from this study:

- The differences between turbid and clean salty waters for the storage zone of the percentage transmissions ($\Delta T\%$) are found to be 10.85 $T\%$ in August, 9.60 $T\%$ in September and 8.80 $T\%$ in October, and the temperatures (ΔT) 10.55 °C in August, 7.5 °C in September and 5.90 °C in October during the three months.
- The turbidity reduces the percentage transmission ($T\%$) and hence the solar radiation reaching the HSZ and the exergy efficiency of the pond.
- The exergy efficiency differences between the clean and turbid salty waters for the HSZ are found to be 6.13% in August, 6% in September and 5.53% in October.

In summary, the exergetic efficiencies are depend on significantly the turbidities of the zones during the three month. Because, the attenuation in the turbid salty water increases more sharply than the clean salty water in the inner zones of the pond. All these effects on the amount of heat storage in the HSZ.

Acknowledgement

The authors acknowledge the support provided by the University of Cukurova under a Grant (Nos. FEF2009D2, FEF2010YL26 and FEF2010BAP5).

References

[1] Saylan L, Sen O, Toros H, Arisoy A. Solar energy potential for heating and cooling systems in big cities of Turkey. Energy Convers Manage 2002;43:1829–37.
[2] Karakilcik M, Dincer I, Bozkurt I, Atiz A. Performance assessment of a solar pond with and without shading effect. Energy Convers Manage 2013;65:98–107.
[3] Sakhrieh A, Al-Salaymeh A. Experimental and numerical investigations of salt gradient solar pond under Jordanian climate conditions. Energy Convers Manage 2013;65:725–8.
[4] Husain M, Patil SR, Samdarshi SK. Simple methods for estimation of radiation flux in solar ponds. Energy Convers Manage 2004;45:303–14.
[5] Wang J, Yagoobi JS. Effects of halobacteria and selected chemicals on radiation transmission in salt water. Sol Energy 1994;52:411–8.
[6] Bryant HC, Colbeck I. A solar pond for London. Sol Energy 1977;19:321–2.
[7] Al-Nimr MA, Al-Dafaie AMA. Using nanofluids in enhancing the performance of a novel two-layer solar pond. Energy 2014;68:318–26.
[8] Hull JR. Computer simulation of solar pond thermal behavior. Sol Energy 1980;25:33–40.
[9] Malik N, Date A, Leblanc J, Akbarzadeh A, Meehan B. Monitoring and maintaining the water clarity of salinity gradient solar ponds. Sol Energy 2011;85:2987–96.
[10] Xu H, Sandoval JA, Lu H, Golding P, Swift A. Operating experience with the El Paso solar pond. In: Joint solar engineering conference. ASME; 1994. p. 503–11.
[11] Wang J, Yagoobi JS. Effect of water turbidity on thermal performance of a salt-gradient solar pond. Sol Energy 1995;54:301–8.
[12] Husain M, Patil PS, Patil SR, Samdarshi SK. Combined effect of bottom reflectivity and water turbidity on steady state thermal efficiency of salt gradient solar pond. Energy Convers Manage 2004;45:73–81.
[13] Karakilcik M, Dincer I, Rosen MA. Performance investigation of a solar pond. Appl Therm Eng 2006;26:727–35.
[14] Butler LRP, Laqua K. Nomenclature, symbols, units and their usage in spectrochemical analysis-IX instrumentation for the spectral dispersion and isolation of optical radiation. Spectrochim Acta B 1996;51:645–64.
[15] Lund PD, Keinonen RS. Radiation transmission measurements for solar ponds. Sol Energy 1984;33:237–40.
[16] Joshi V, Kishore VVN. A numerical study of the effects of solar attenuation modelling on the performance of solar ponds. Sol Energy 1985;35:377–80.
[17] Kirk J. Spectral absorption properties of natural water's contribution of the soluble and particulate fractions to light absorption. some inland waters of South Australia. Aust J Mar Freshwater Res 1980:31 287–296.
[18] Li YX, Kanayama K, Baba H. Spectral calculation of the thermal performance of a solar pond and comparison of the results with experiments department of mechanical engineering. Renewable Energy 2000;20:371–87.
[19] Rabl A, Neilsen CE. Solar ponds for space heating. Sol Energy 1975;17:1–2.
[20] Holman JP. Heat transfer. 8th ed. McGraw-Hill; 1997.
[21] Tsilingiris PT. Radiation transmission through a composite pure water layer of uniform and depth-dependent extinction characteristics. Int J Energy Res 1991;15:723–30.
[22] Dincer I. The role of exergy in energy policy making. Energy Policy 2002;30:137–49.
[23] Hawlader MNA. The influence of the extinction coefficient on the effectiveness of solar ponds. Sol Energy 1980;25:461–4.
[24] Petela R. Exergy of undiluted thermal radiations. Sol Energy 2003;74:469–88.
[25] Sun H, Feistel R, Kochm M, Marko A. New equations for density, entropy, heat capacity, and potential temperature of a saline thermal fluid. Deep Sea Res I Ocean Res Pap 2008;55:1304–10.
[26] SPSS, Computer program. MS for Windows. Version 15.0. USA: SPSS Inc.; 2006.